

## **Systematic Errors of the CWB Global Forecast Model Part I: Fundamental Variables and Mean Meridional Circulation**

JOUGH-TAI WANG<sup>1</sup>, WEN-MEI CHEN<sup>2</sup>, and SONG-CHIN LIN<sup>1</sup>

(Manuscript received 31 August 1992, in final form 18 February 1993)

### **ABSTRACT**

The Central Weather Bureau (CWB) of the Republic of China officially began its NWP operation on July 1, 1988. The global forecast model at CWB is a multi-level grid point model with fourth order potential enstrophy conservation scheme in the horizontal differencing. Based on the forecast data, January and July model climatology from the day-1, day-2, and day-3 forecasts are constructed. Also the simulated mean meridional circulation are investigated. The systematic errors can be identified by comparing the model climatology with the observed analyses.

For the January simulation from day-1 forecast of the height field, it is found that the strength of the Aleutian low and the Siberian high are all underestimated. Day-2 and day-3 forecasts show further decrease in intensity of those two dominant systems. The temperature simulation at 850 hPa level indicates that negative mean bias exists in most of the land area in Asia, while positive bias prevails in the oceanic region. The 500 hPa height field from day-1, day-2 and day-3 simulations all indicate that large negative biases are around southwestern China mountain ranges. In July, the Pacific high is well reproduced in those three forecasts, and the mean bias related to the land-ocean contrast is reduced. The Pacific high shrinking in its N-S range and extending further westward can be identified in the July climatology from day-2 and day-3 forecasts.

Zonal mean structures of the zonal wind and meridional wind in January and July reveal the model's ability to capture the seasonal migration of the general circulation. Day-2 forecast gives better Hadley cell simulation compared with the day-1 forecast.

The systematic errors from the CWB model are compared with the errors of other operational models (*e.g.*, ECMWF, NMC). The implications of those mean errors are also discussed.

---

<sup>1</sup> Institute of Atmospheric Physics, National Central University, Chung-Li, Taiwan 32054, R.O.C

<sup>2</sup> Central Weather Bureau, Taipei, Taiwan 10039, R.O.C

## 1. INTRODUCTION

After Richardson (1922), the very first successful numerical weather prediction (NWP) experiment was conducted by Charney, Fjortoft and von Neuman at 1950. In their paper (Charney, *et al.*, 1950), a barotropic non-divergent vorticity equation was used to forecast the movement of 500 hPa height field. During that experiment, a low pressure system movement due to advection was well captured. Phillips (1956) was among the first to use a baroclinic model to conduct a forecast experiment. Phillips' experiment also enjoyed some successes, however, the model blew up after more than twenty days' integration due to the later identified effect of nonlinear instability (Phillips, 1959).

The NWP has come a long way from that start. Rapid progress in the main components of the NWP system have been witnessed. From the NWP model itself, a full three dimensional primitive set of equations was widely used as the community's prototype operational model. For the numerical aspects, the famous schemes used in the earlier days, such as the Arakawa Jacobian (Arakawa, 1966), the staggered Arakawa grid with energy conservation (Arakawa, 1972), TASU (Time Alternating Space Uncentered) scheme (Arakawa, 1972). Nowadays, the popular schemes are the potential enstrophy conserving (Arakawa and Lamb, 1981), the semi-implicit time scheme and spectral transform techniques (Bourke, 1972). The introduction of the semi-implicit scheme is to speed up the calculation. The concept of spectral method (Williamson and Dickinson, 1976) was adopted for its exactness in spatial representation. Both the NMC (National Meteorological Center) of the USA and ECMWF (European Center of Medium-Range Weather Forecast) now use the spectral model.

For the treatment of the initial data for forecasting purpose, it went through the simple Barnes objective analysis to the very sophisticated diabatic/adiabatic nonlinear normal mode initialization for the spectral model (Williamson and Dickinson, 1976), or the dynamic balanced initialization for the finite difference model at present time. For error checking and quality control of the station data, from the simple gross error check to the sophisticated CHQC (Comprehensive Hydrostatic Quality Control) methodology was adopted as in NMCmodel (Kalnay, *et al.*, 1990).

In the area of the parameterization of the sub-grid scale processes, there also is much progress. In order to represent the thermodynamic effect of the sub-grid scale process, Kuo (1974) used the existence of low-level moisture convergence as a criteria to identify its contribution. Anthes and others followed Kuo's approach and modify some of the parameters to accommodate wider range of physical conditions. This type of formulation was also adopted in some of the regional models. During the same period, Arakawa and Schubert (1974) proposed another way of representing the sub-grid scale's thermodynamic effect. Arakawa and Schubert (1974) assumed that sub-grid scale process can be represented by the ensemble of cumulus cloud. In their formulation, the cumulus cloud is small compared to the large-scale environment, however, it is not negligible. And the governing equation of the cumulus ensemble can be established, with some assistance of the cloud model. They then proposed the idea of "quasi-equilibrium" to serve as the closure assumption for the thermodynamic aspects of cumulus parameterization. The cloud model adopted in Arakawa and Schubert (1974) only had a convective updrafts component.

After GATE (GARP Atlantic Tropical Experiment) in 1974, it was identified that for a tropical cloud, it usually appeared in a cluster fashion, not in a single cloud as envisioned by Arakawa and Schubert (1974). For a cloud cluster system, it usually contained mesoscale system with sizable updrafts and downdrafts. The findings revealed that for a large scale NWP model, the sub-grid scale processes should include not only the convective updrafts and downdrafts, but also the meso-scale updrafts and downdrafts. The study by Johnson

(1984) indicated the potential importance of mesoscale components in contributing to the large-scale heating profile.

Yanai *et al* (1973) pointed out that only considering the convective updrafts in the parameterization would tend to cause the atmosphere to be too dry, due to the excessively-induced large-scale subsidence. Cheng and Yanai (1989) succeed in incorporating the convective downdrafts in the cloud model used to parameterize the cloud thermodynamics effect. And the result from Cheng and Yanai (1989) indeed indicated the inclusion of convective downdrafts in the parameterization reduced the large-scale drying effect, at least clearly in 600–800 hPa level.

With all the improvement in the model numerics, physics and initialization, the operational NWP model performed fairly well, as revealed by the anomaly correlation. People usually regards the day of anomaly correlation reaching 60% as the limit of a meaningful forecast. For example, for the NMC and ECMWF models, their anomaly correlation reached 60% at day 6, which was an increase of about 1 to 2 days compared to the older version of the models (Brankovic *et al.*, 1990; Kalany *et al.*, 1990)

As revealed by the foregoing discussions, an operational NWP forecast contains several important modules (i.e., the numerics, the model physics, the initial data and initialization,... etc.). Each module is an important issue itself for continuing improvement. In view of this rapid development, the Central Weather Bureau (CWB) of the Republic of China officially began its operational NWP forecast on July 1, 1988. Since then, several models had been run routinely to provide the forecast up to five days.

The operational system for the CWB now includes the global, regional, and limited area models. The salient features of the CWB global model are briefly discussed here. The global forecast model at CWB is a multi-level grid point model with fourth order potential enstrophy conservation scheme in the horizontal differencing. The model has a horizontal resolution of  $2.4^\circ$  by  $3.0^\circ$  and is in Arakawa staggered "C" grid with nine vertical sigma levels between the surface and 50 hPa. The Arakawa and Schubert (1974) cumulus parameterization, the Randall-Deardorff well-mixed planetary boundary layer parameterization, the Katayama (1974) formulation of radiative transfer and the ground hydrology calculation by Arakawa and Mintz (1974) are all included in the model's physical parameterizations. This model is integrated for up to five days to provide the global forecast (Liou *et al.*, 1989).

Based on the simulated data of the past four years, the objective of this paper is to identify the systematic errors existing in the CWB global forecast model and also the processes related to the errors. Since an operational NWP simulation contains several different modules, it is then quite difficult to point out a simple module which is solely responsible for causing the model errors. However, in this study, we will try to identify the processes that potentially could be related to the causes of the errors.

Part I of this study focussed on the performance of the zero order moment of the global model. Namely, the simulation structures of the fundamental variables and the behavior of the mean meridional circulation (MMC). The simulated results are also compared with the observed structures and other operational models. The main goal of this study in Part I is to document the performance of the model behavior. Part II of this paper will then discuss the structure of higher-order moment, which include the investigation of the energetics characteristics of the CWB global model. Based on this higher order moment analysis, not only the salient model features can be identified, but also it is plausible to speculate about processes potentially related to the causes of the systematic errors with more evidence.

## 2. DATA

The CWB global forecast system performed forecast of up to five days from 0000 UTC and 1200 UTC, with a wait of three hours for data arrival. Based on the output data stored, the simulated monthly mean climatology of day-1, day-2 and day-3 forecast are calculated solely from the model's output with twice daily simulated data. The CWB global forecast model has horizontal resolution of  $3^\circ$  by  $2.4^\circ$ , with nine vertical levels in the  $\sigma$  coordinate. The adiabatic time integration is 2.5 minutes and the diabatic integration is every 45 minutes.

The systematic errors are identified as the difference between the simulated model climatology and the observed climatology. The observed climatology can be established from the post objective analysis of observed data. For Part I of this study, the monthly mean climatology of fundamental variables are thus constructed. The surface pattern, along with the middle and upper-level structures of the simulated fields are compared with the observed and with other model results. The zonal mean structure of the meridional wind field ( $v$ ) are used to identify the MMC (i.e., the Hadley cell and Ferrel cell) and its seasonal reversal. And the MMC structures are also a good way to highlight the model's performance.

Due to the data limitation, in this study we only investigate the systematic errors for the months of July 1989 and January 1990. The results are only for those two individual months, and is not a composite type of study. From now on in the rest of this paper, the meaning of the day-1 simulation means the monthly simulated climatology, constructed solely from all the day-1 forecasts of that month, either for January or July. The terms of day-2 and day-3 simulation have the same implied meaning.

## 3. RESULTS AND DISCUSSIONS

### 3.1 Horizontal Structures for January

The dominating systems for the January surface pressure structure are the Aleutian low, the Siberian high and the Icelandic low. Figure 1 shows the January simulation of the surface pressure from day-1, day-2 and day-3 simulations. The positions of the Aleutian low and the Siberian high are simulated well in the climatology constructed from the day-1 forecast, but the intensity of those systems are underestimated slightly. Day-2 and day-3 forecasts show further decrease in the intensity of those two dominant systems.

The 500 hPa height field bias (the simulated minus the observed) from day-1, day-2 and day-3 simulations, as shown in Figure 2, all indicate that there exist large negative bias in the Asia continent, while positive bias prevails in the oceanic region. For 500 hPa height field, the mean condition is that the Pacific high system situated to the southeast of Taiwan (in the oceanic region). The positive height bias of the CWB model in the oceanic region reveals that the intensity of the high at that level is over-estimated.

The temperature field at 1000 hPa level indicates that the forecast values are too cold. The temperature bias around Taiwan area is on the order of  $5^\circ\text{C}$ . Figure 3 represents the temperature fields at 850 hPa level. The forecast fields tend to have negative (positive) temperature bias in the mainland (oceanic region). However, these bias structures are different from those at 500 hPa and 300 hPa levels. Figure 4 shows 500 hPa level temperature bias for January. For those three simulated climatologies at that level, all tend to have positive bias. This indicates that the forecast temperatures are too warm in most of the places.

Wind vector biases at 700 and 300 hPa levels, shown in Figure 5, indicate that the 700 hPa level tends to have southwest component in Asia and W. Pacific, while the bias at 300 hPa level possesses a northeast component. The simulated wind vector at those levels have

different vertical bias structures, and this could be related to the different horizontal structure of temperature bias. The intensity of the jet for day-1 forecast of January at 200 hPa level is well simulated. The bias distribution for that level is quite similar to those at 300 hPa level. However, the position of the jet core is shifted about several degrees towards the northeast. Day-2 and day-3 simulated data indicate further northeastward shift of the jet core (figures not shown).

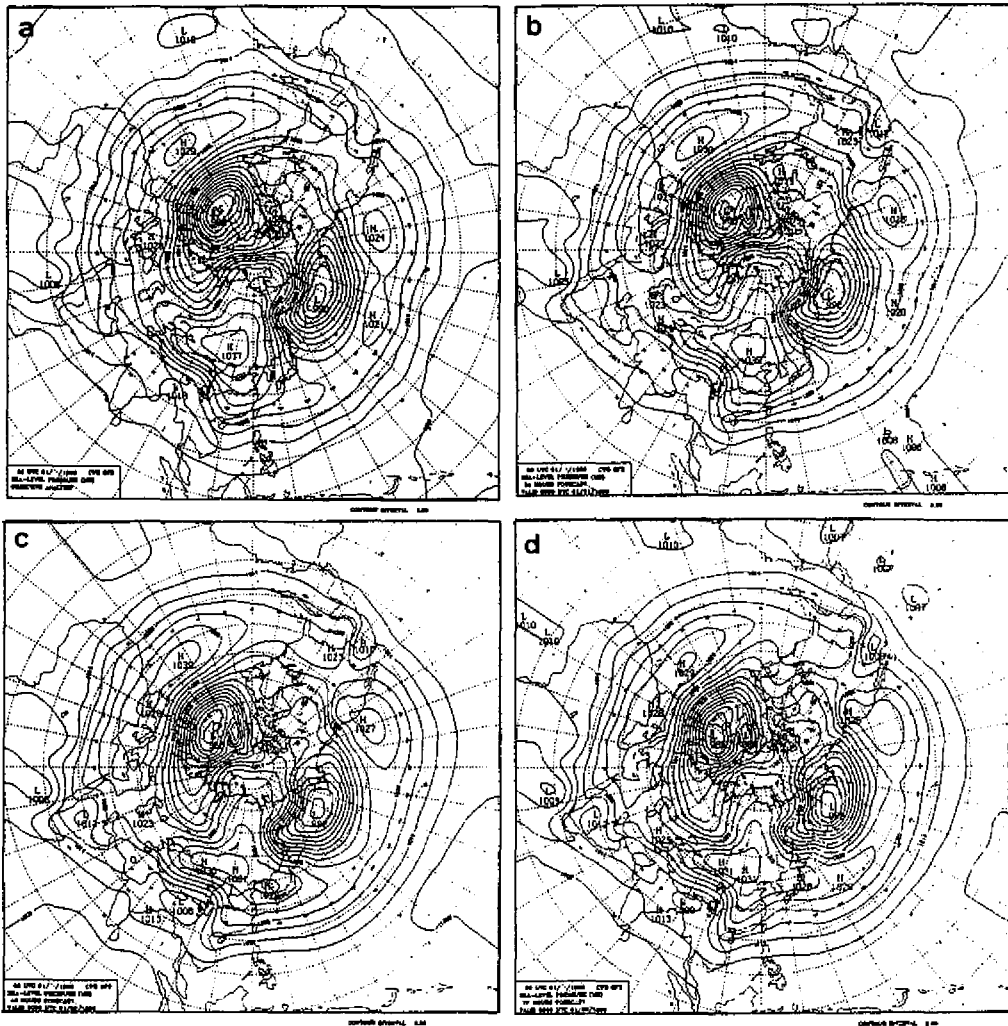


Fig. 1. The monthly mean sea level pressure for January 1990. (a) observed field, (b) day-1 forecast, (c) day-2 forecast, (d) day-3 forecast.

### 3.2 Horizontal Structures for July

In July, the dominating system in the Eastern Hemisphere is the Pacific high and the monsoon trough in the Asian continent. For July simulation of the sea level pressure shown in Figure 6, the Pacific high is well reproduced in those day-1, day-2 and day-3 forecasts. This is a good indication that the model can capture the seasonal reversal of the dominating system. The mean bias related to the land-ocean contrast is smaller than those from January simulation. Figure 7 indicates the distribution of height field at the 500 mb level. The simulated Pacific high shrinking in its north-south range and extending further westward can be identified in the simulated July climatology from day-1 and day-2 forecasts. The July temperature bias at 1000 hPa level in the Asia region are all too cold, quite similar to the January error structure. The temperature simulation at 500 hPa level through the day-2 forecast (Figure 8) indicates positive bias in the East Asia land area, and negative bias in the ocean region southeast of Taiwan.

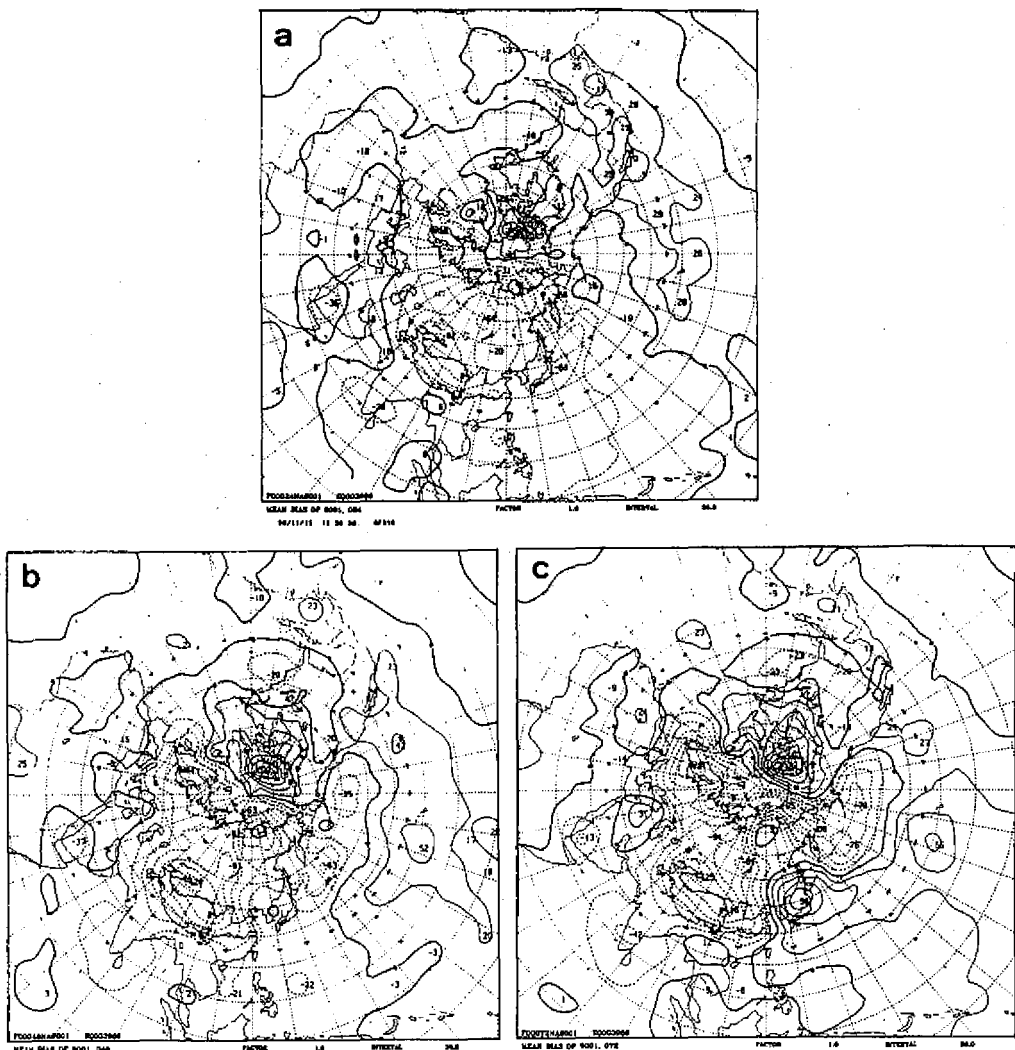


Fig. 2. The height field bias (forecast-observed) at 500 hPa level for January 1990. (a) day-1 forecast, (b) day-2 forecast, (c) day-3 forecast.

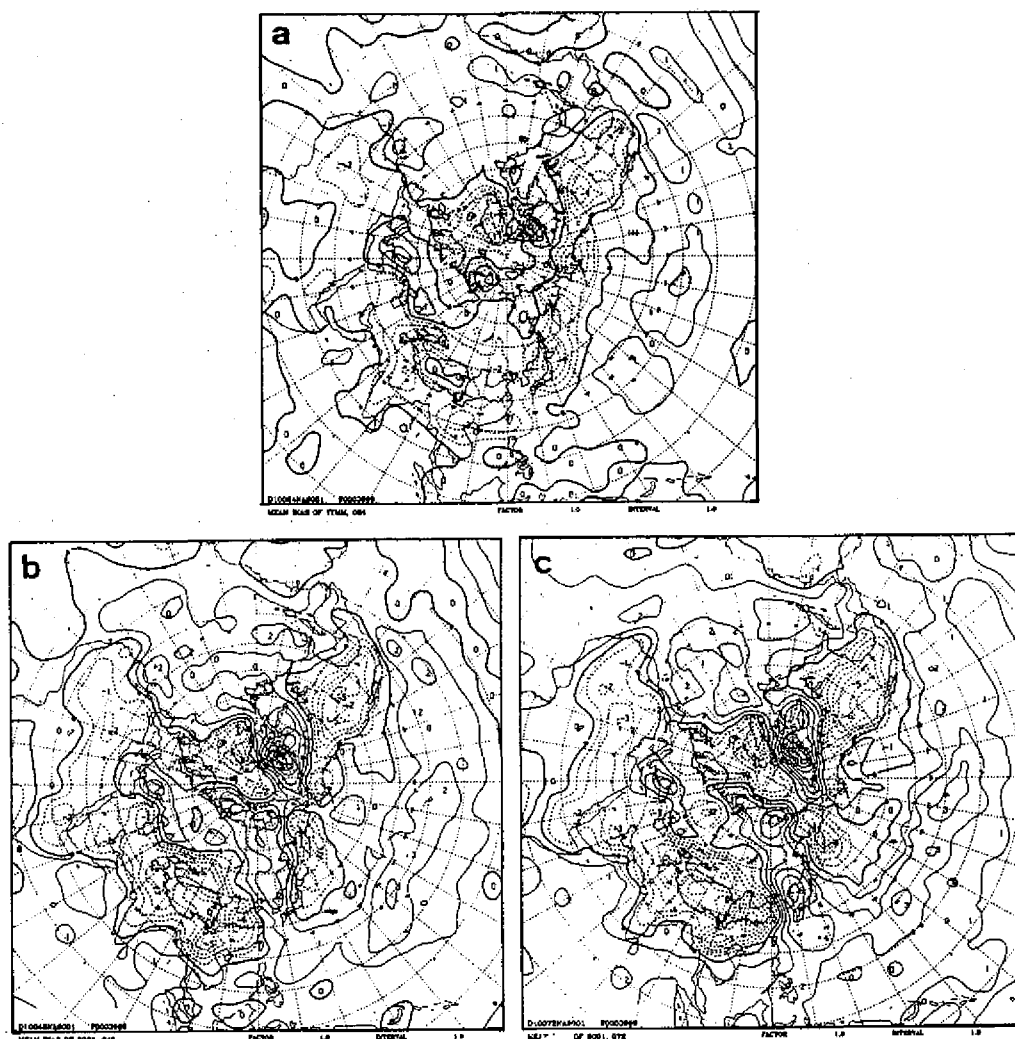


Fig. 3. The temperature bias at 850 hPa level for January 1990. (a) day-1 forecast, (b) day-2 forecast, (c) day-3 forecast.

### 3.3 Zonal Mean Structures

Figure 9 indicates the simulated January zonal mean structure of the zonal wind in the Northern Hemisphere (NH) from the day-1 and day-2 forecast. The corresponding observed features are shown in Figure 10. The intensity and position of the subtropical jet are well simulated in both the day-1 and day-2 simulated climatology. The simulated and observed zonal mean of the meridional wind distribution in the NH is presented in Figures 11 and 12, respectively. These figures can be regarded as a measure of the mean meridional circulation (MMC). For the winter time, the thermal equator (the area with maximum rising motion) is

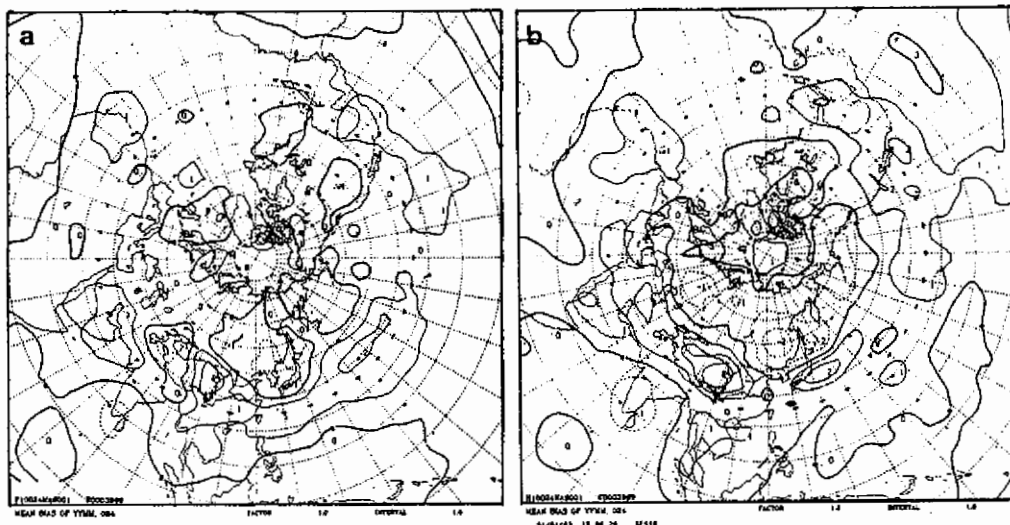


Fig. 4. The temperature bias for day-1 forecast of January 1990. (a) 500 hPa level, (b) 300 hPa level.

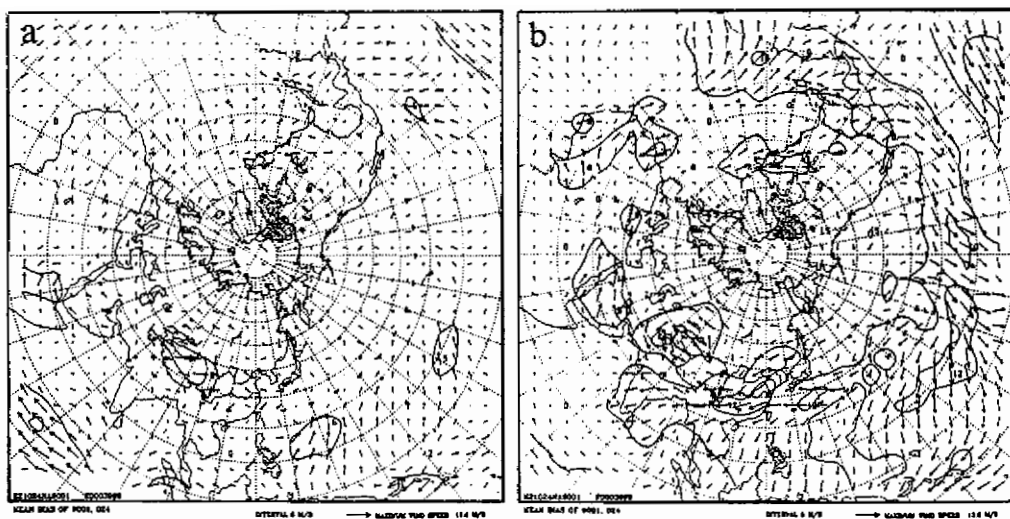


Fig. 5. The wind vector bias for day-1 forecast of January 1990. (a) 700 hPa surface, (b) 300 hPa surface.

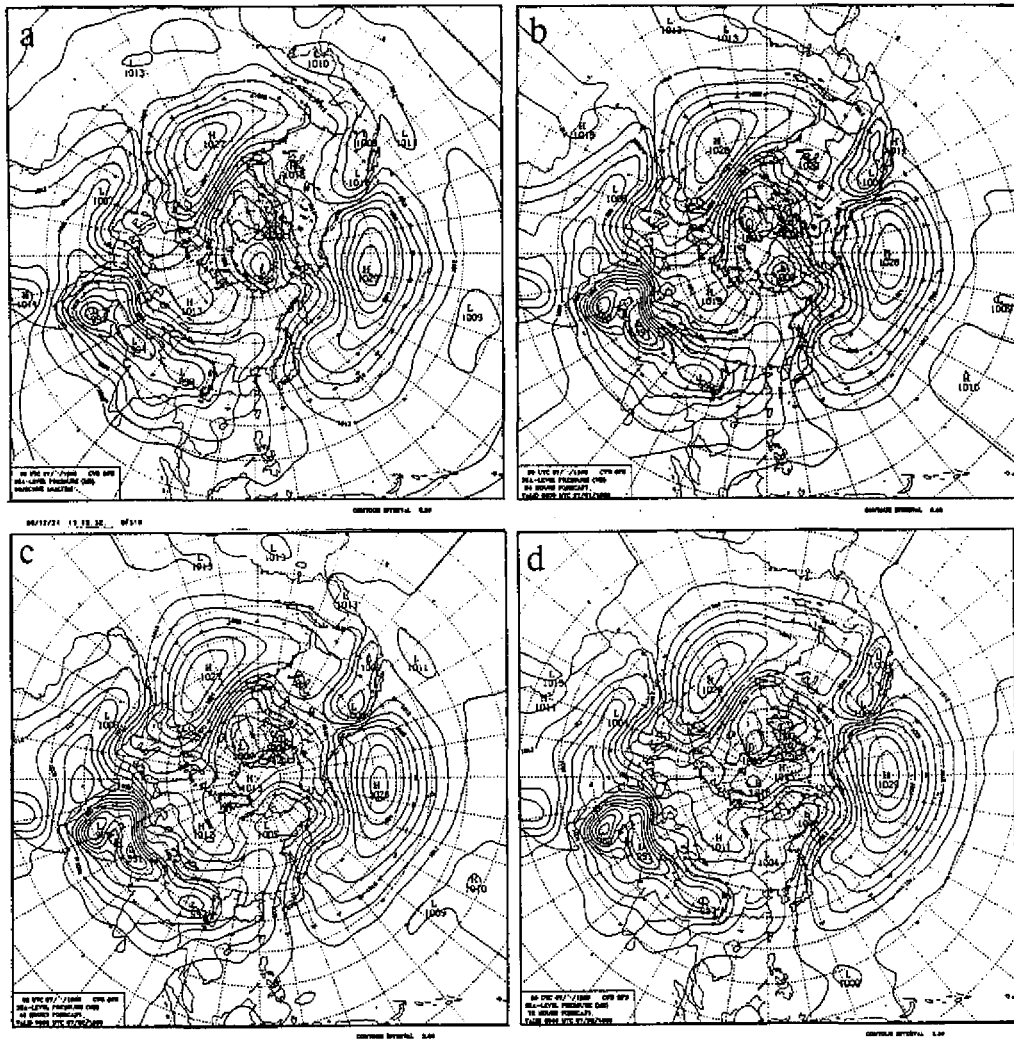


Fig. 6. Same as Fig. 1, except for July 1989.

in the Southern Hemisphere (SH) around  $5^{\circ}S$  to  $10^{\circ}S$ , and the sinking branch of the Hadley cell, which produces the subtropic high is around  $20^{\circ}N$ . The Hadley cell simulated by the day-1 climatology is quite shallow, only up to 600 hPa. There also is an erroneous southward transport of mass toward the equator at upper-level. Low-level divergence indicates the subsiding air is simulated to be around  $30^{\circ}N$ , which is too far north (about  $10^{\circ}$  of latitude).

The day-2 simulation behaves better than the day-1 simulation. The Hadley cell is deeper, but its intensity is still too weak. The subtropic high is also simulated to be too far north (as in day-1 case), in comparison with the observed distribution. The Ferrel cell indicated in the observed January climatology is also quite weak. However, in the day-1 and day-2 simulation, the Ferrel cell can still be identified. The reason day-2 simulated Hadley cell develops better is that we suspect for longer integration time (up to 48 hours) the model

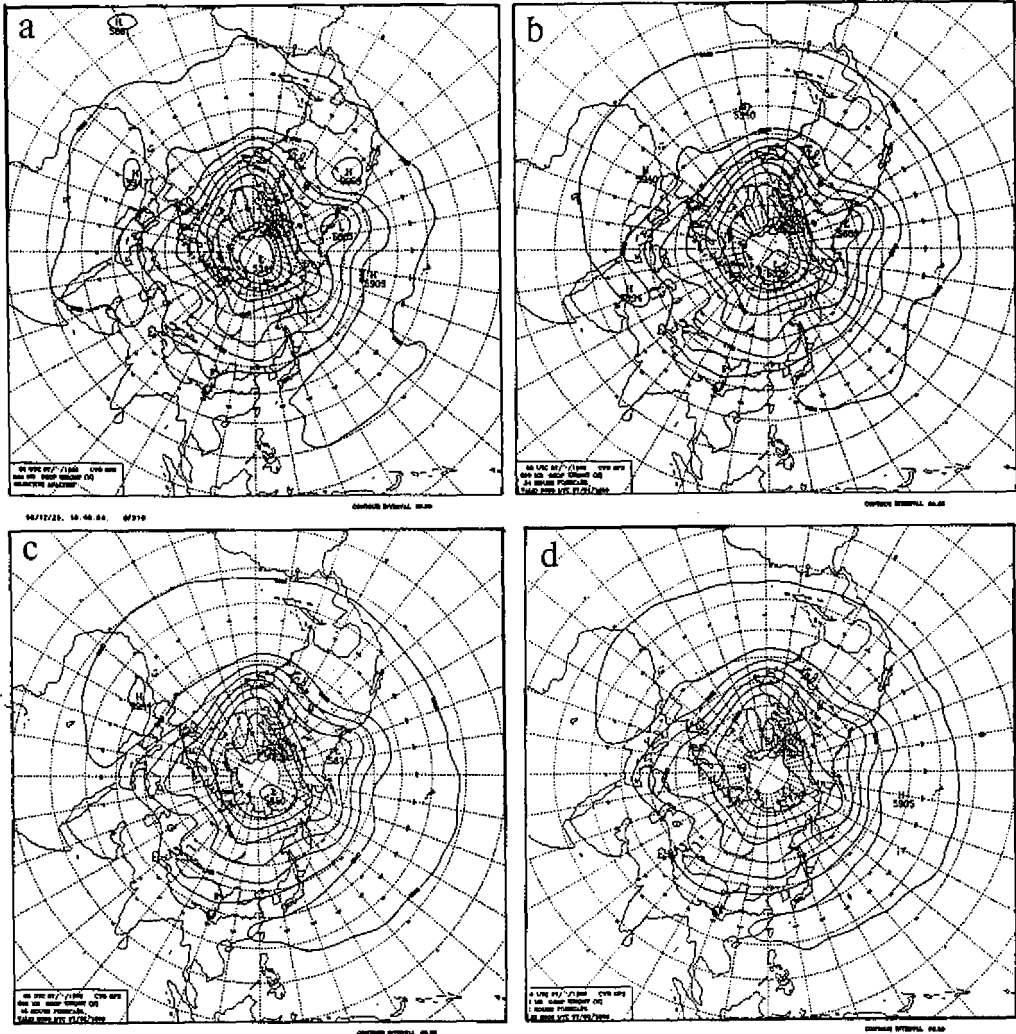


Fig. 7. Same as Fig. 1, except for 500 hPa level of July 1989.

physics have enough time to do the mutual adjustment and are capable of producing more realistic distributions. Figure 13 shows the zonal mean of the temperature bias (simulated minus the observed) distribution. For the January day-1 forecast, it reveals that the simulated zonal mean temperature is too warm. In the tropics, the zonal mean temperature bias for the day-2 shows the negative distribution at low-level, while the middle to upper level possess a positive distribution. This tendency tends to increase the static stability of the model atmosphere. This situation reverses in the higher latitude. However, Arpe and Klinker (1986) described that temperature bias in the ECMWF model decrease the model's static stability. This is quite opposite to the present CWB model.

The zonal mean of the zonal wind for July simulation from day-1 and day-2 forecast, along with the observed feature are presented in Figures 14 and 15, respectively. The shift of the jet maximum in the subtropics to  $45^{\circ}N$  is also simulated well. Again, the seasonal

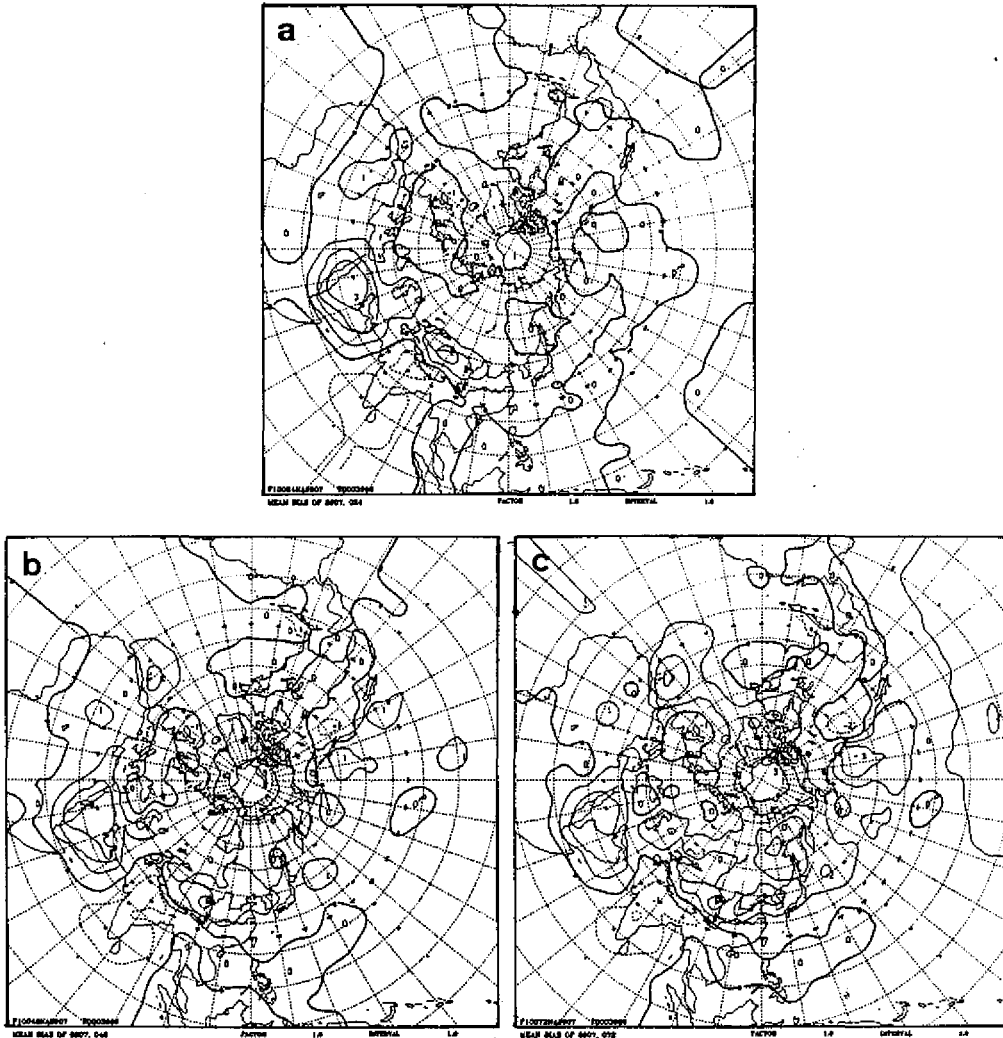


Fig. 8. The temperature bias at 500 hPa level for July 1989. (a) day-1 forecast, (b) day-2 forecast, (c) day-3 forecast.

migration of the general circulation can be captured well by the model. The simulated and observed zonal mean of the meridional wind are presented in Figures 16 and 17, respectively. For the observed zonal features, the upper-level divergence associated with the Hadley cell occurred around  $15^{\circ}N$ , and the low-level convergence is not obvious. The day-1 simulated field revealed that the weak low-level convergence for the Hadley cell occurred around  $26^{\circ}N$ , while the upper level divergence occurred at  $20^{\circ}N$ . For the day-2 simulation, results indicate the low-level convergence is around  $10^{\circ}N$ , and the upper-level divergence is way up to around 250 hPa and quite weak. The ITCZ is simulated to a further south position in day-2 simulation, while it is simulated too far north in day-1 case. The implications of erroneous

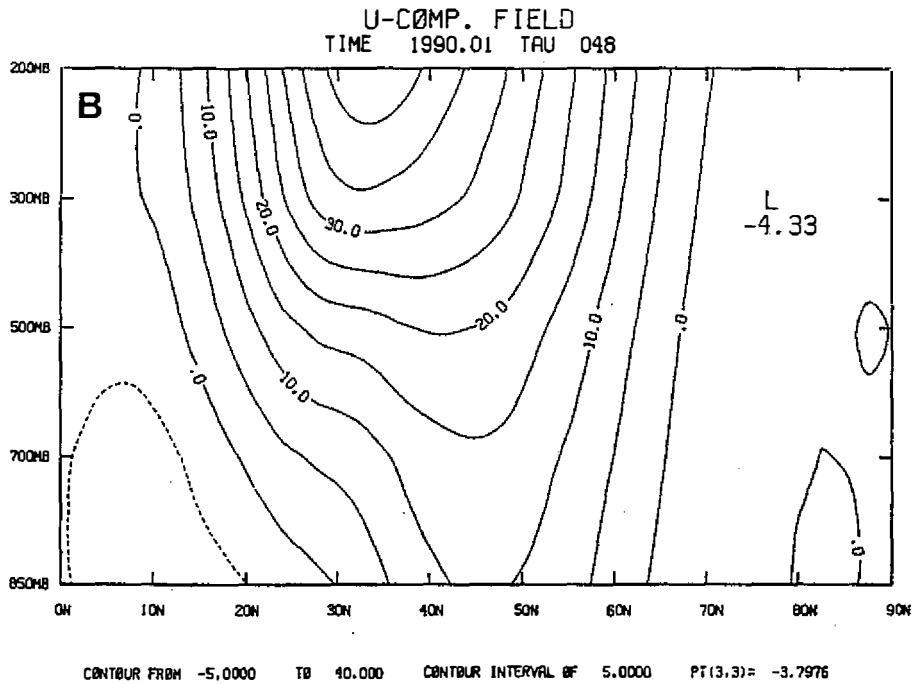
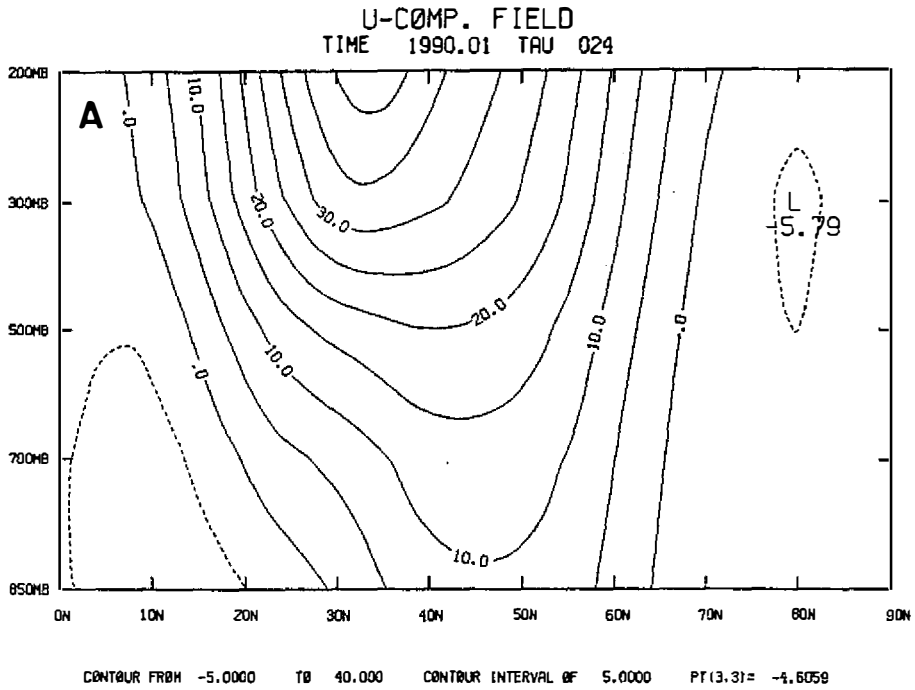


Fig. 9. The simulated zonal mean of the zonal wind for January 1990 in the Northern Hemisphere. (a) day-1 forecast, (b) day-2 forecast.

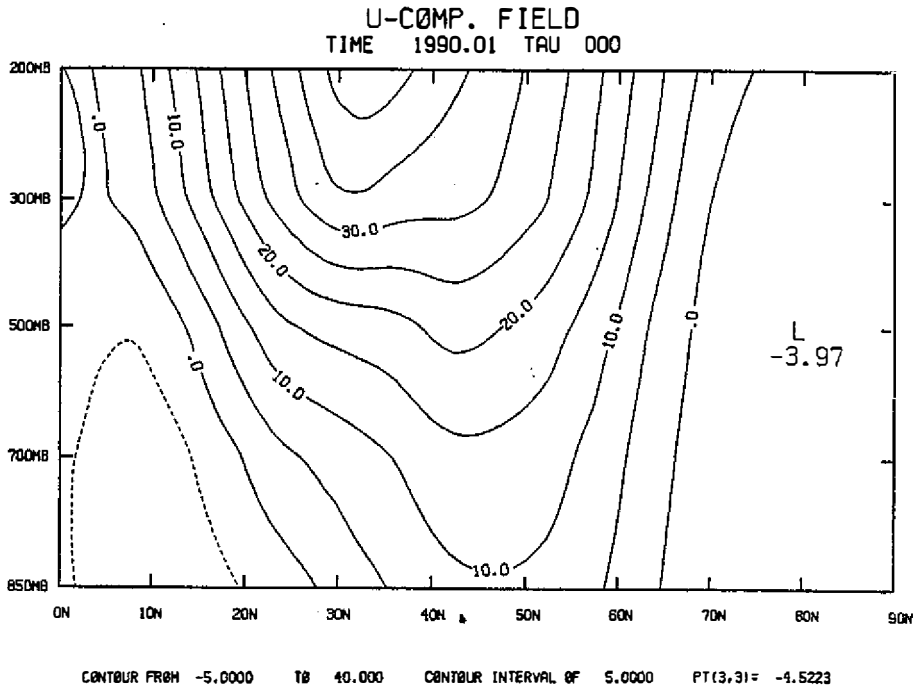


Fig. 10. The observed zonal mean of the zonal wind for January 1990.

ITCZ position will be discussed later. Figure 18 is the same as Figure 13, except for the July simulation. The negative temperature bias at lower-level and positive bias at upper-levels are clearly indicated. This structure is similar to the January simulation.

### 3.4 Discussions and Comparisons

From the horizontal structures of the January and July simulations, it is indicated that the CWB model is capable of reproducing the seasonal migration of the general circulation, also the jet core and other salient features. The January simulation reveals that the intensity of the Siberian high and the Aleutian low are underestimated in the model for all the simulations. The position of the subtropics high simulated in January, as represented by the zonal mean of the zonal wind, shift too far north, compared with the observed. The July simulation of the ITCZ is far too south for day-2 simulation. Based on this analysis, we know then the CWB model in January has the tendency to produce a wetter climate in the East Asia region. In July, however, the model has the tendency of producing drier simulated climatology in East Asia for its day-2 simulation. The shift of the simulated ITCZ position should reflect its characteristics in the energetics structure. The general consensus is that the usage of observed sea surface temperature (SST) in the oceanic region plays a role in affecting the surface pressure simulation.

As indicated in Figure 2, the 500 hPa level pressure simulation has the tendency to produce a negative bias in the Asia continent, along with a positive bias in the oceanic region. Bettge (1983), based on the NMC and ECMWF data, studied the simulated monthly

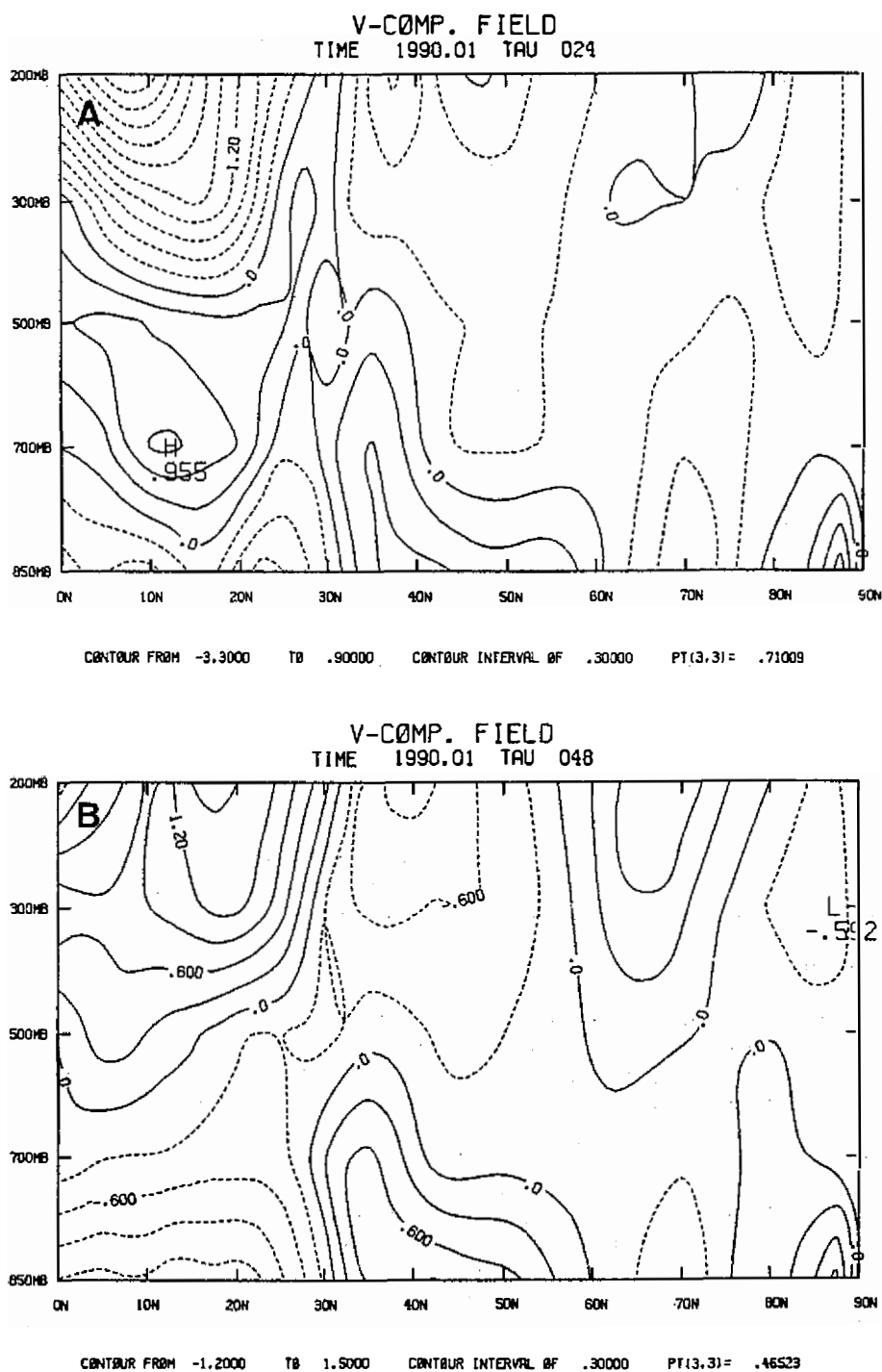


Fig. 11. The simulated zonal mean of the meridional wind for January 1990 in the Northern Hemisphere. (a) day-1 forecast, (b) day-2 forecast.

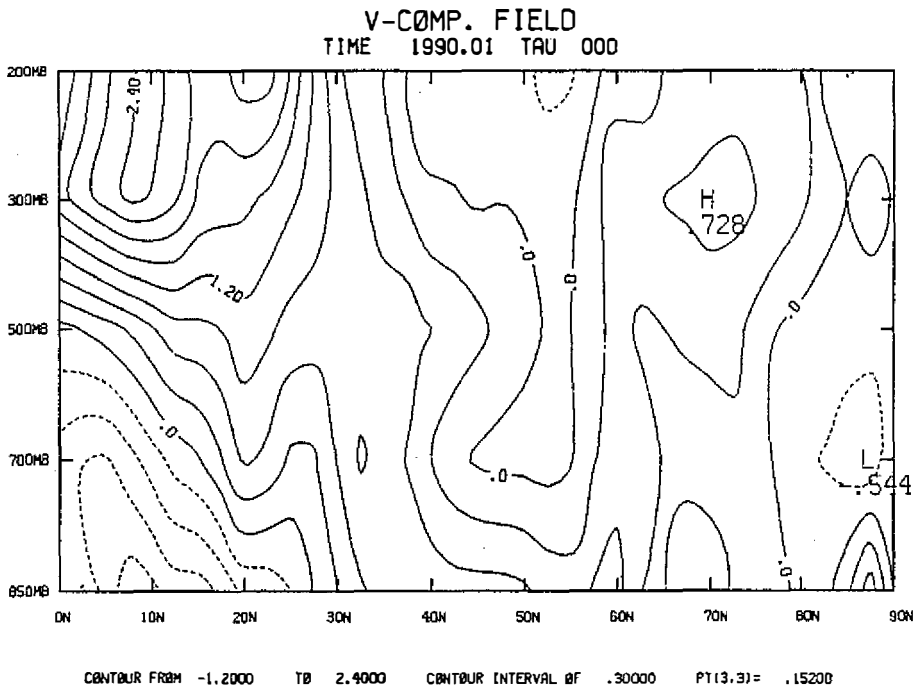


Fig. 12. Same as Fig. 10, except for the observed meridional wind.

climatology from a 24 hr forecast. It was found that for 500 hPa height field, these models also indicate a positive bias over the Pacific and a negative bias over land area. The CWB model has similar bias structure. Wallace *et al.* (1983) used the ECMWF model to investigate the way to reduce this systematic error. It was suggested that an envelope orography be included in the model bottom topography in order to reduce the systematic error due to the land-sea contrast. The investigation by Tibaldi (1985) seemed to support their suggestion. However, this study found that the inclusion of an envelope orography just reduced the intensity of the systematic errors, the east-west error lack of homogeneity still exists. These points deserve more study.

Zonal mean structure of the January simulation also captures the main seasonal change of the MMC. The erroneous southward transport of the Hadley cell will decrease the mass of the Northern Hemisphere. Weak Ferrel cell in the mid latitude reflects the baroclinic eddies intensity is underestimated. This is related to the simulated static stability structure in the lower troposphere as indicated in Arpe and Klinker (1986).

The vertical structure of the temperature bias for the CWB model indicates positive bias in the middle troposphere and negative bias in the lower troposphere. This tendency increases the static stability for the lower troposphere. For the ECMWF model, the static stability was decreased through the simulated temperature structure as discussed in Arpe and Klinker (1986). The implication is that the Ferrel cell development is too strong with the weaker static stability as in ECMWF's model. However, in the present model, the increase in static stability causes the decrease in the intensity of the Ferrel cell.

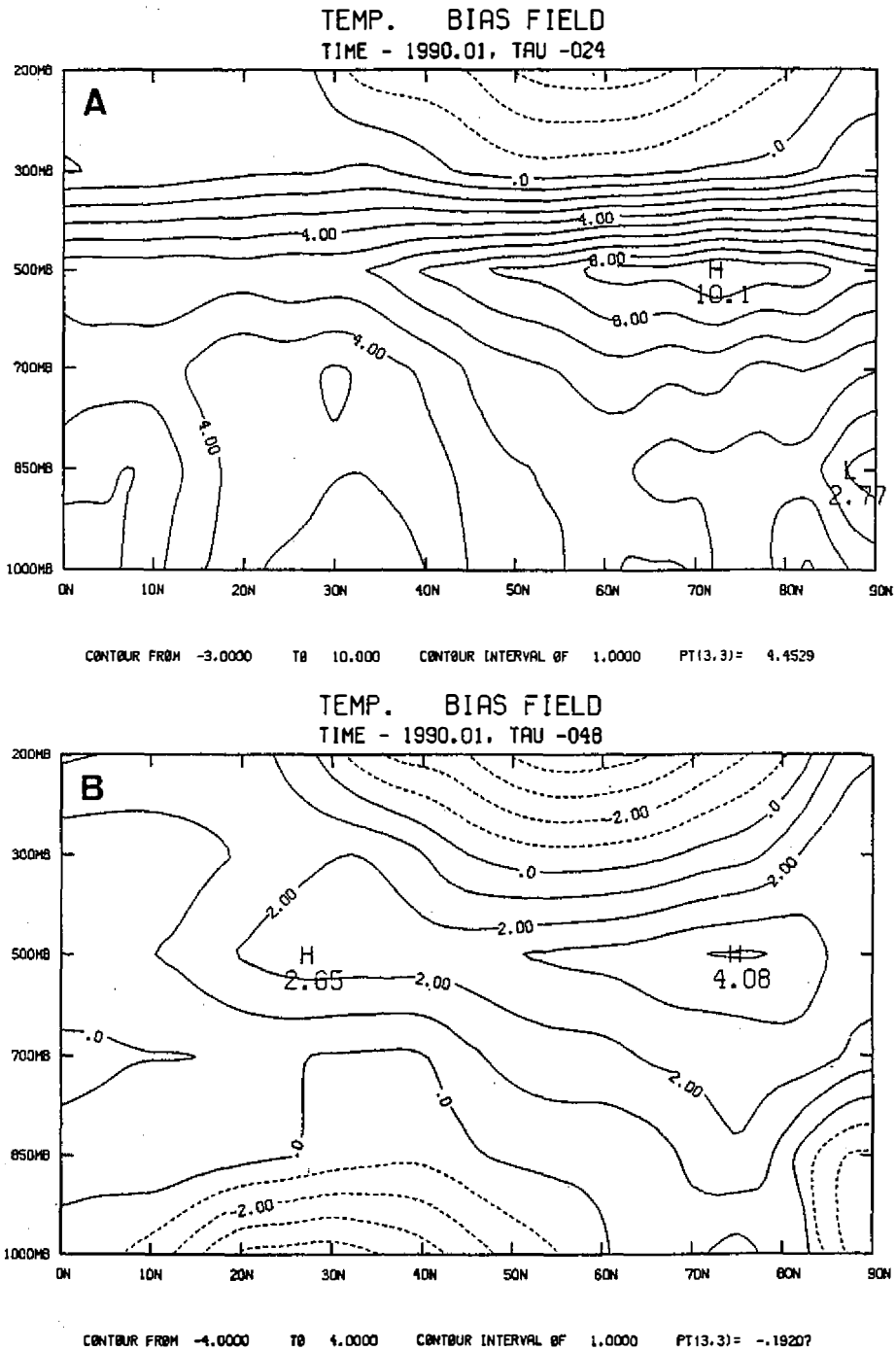


Fig. 13. The zonal mean of the temperature bias for January 1990. (a) day-1 forecast, (b) day-2 forecast.

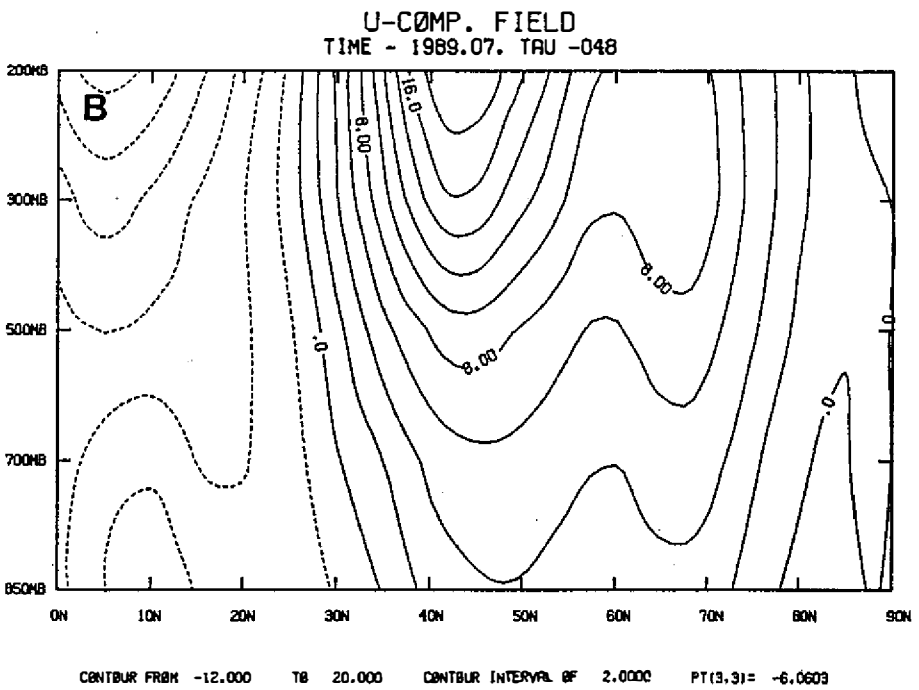
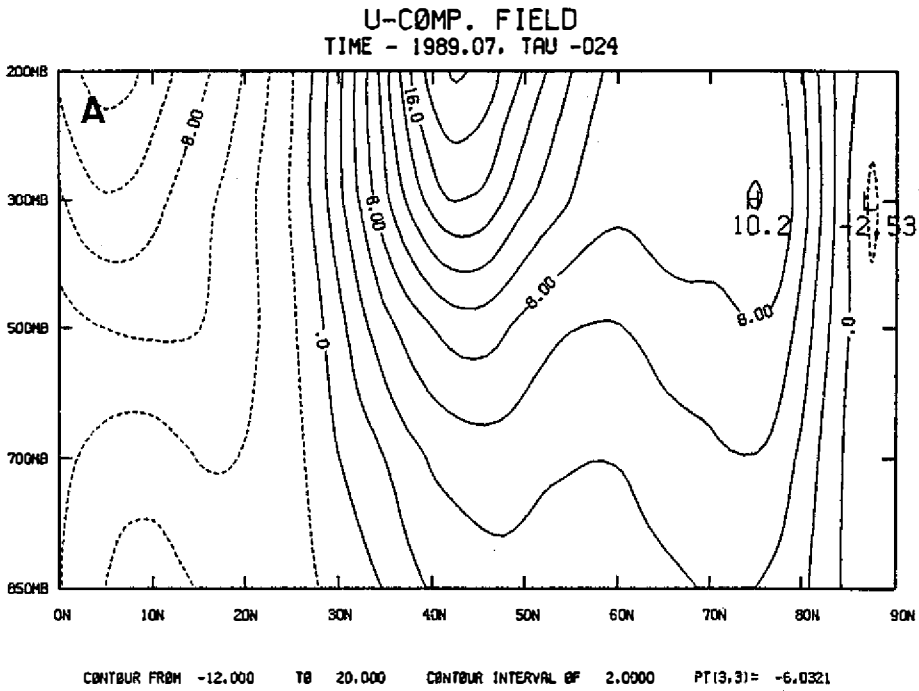


Fig. 14. Same as Fig. 9, except for July 1989. (a) day-1 forecast, (b) day-2 forecast.

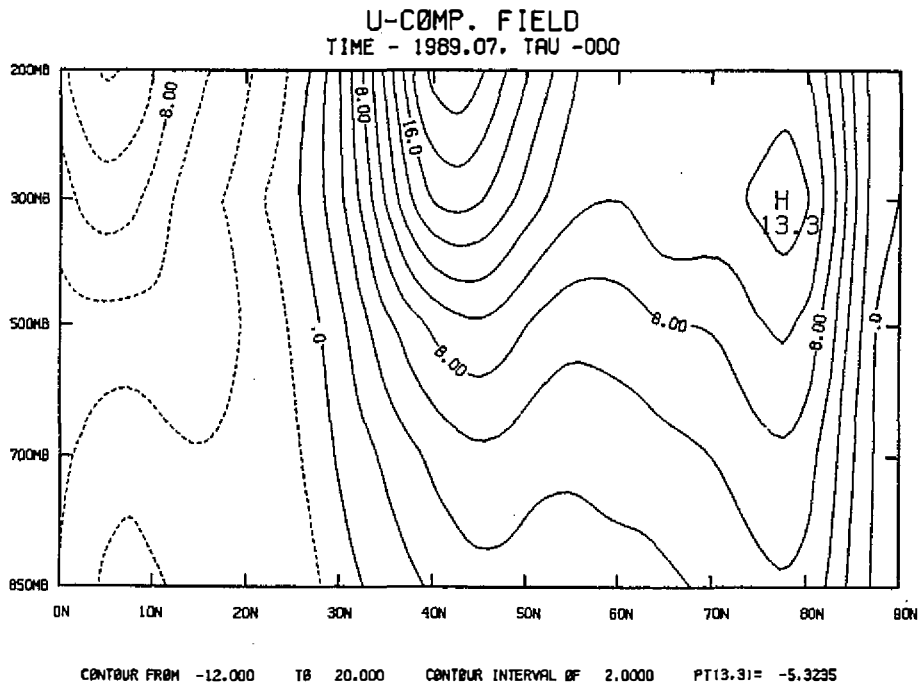


Fig. 15. Same as Fig. 10, except for July 1989.

The deficiency in the surface temperature simulation over land may be attributed to the parameterization of the land surface processes. Pan (1990) pointed out that a change in the formulation of the surface evapotranspiration scheme provided better surface simulation of the NMC medium range forecast model. This is one of the area the CWB model can perform more study.

Kalnay *et al.* (1990) discussed the NMC forecast model performance. They found that, for the mean surface precipitation in the winter time, the relative large precipitation in Asia occurred around the western Pacific ocean to the east of  $120^{\circ}\text{E}$  and extended toward the southwest. The CWB January day-1, 2 and 3 forecasts (Figure 19) of the mean precipitation also indicate the same feature. Although this result hasn't been compared with the observed precipitation field, the feature of southwest extension of large surface precipitation is found to correspond to the regions of the relative minimum of the outgoing longwave radiation.

#### 4. SUMMARY AND CONCLUDING REMARKS

Based on the forecast data from the CWB model, January and July model climatology from the day-1, day-2, and day-3 forecasts are constructed. Also the simulated mean meridional circulation are investigated. The systematic errors can be identified by comparing the model climatology with the observed analyses.

In conclusion, we found that the CWB global forecast model can reproduce the dominant features for January and July, with the tendency to underestimate its intensity. Zonal mean

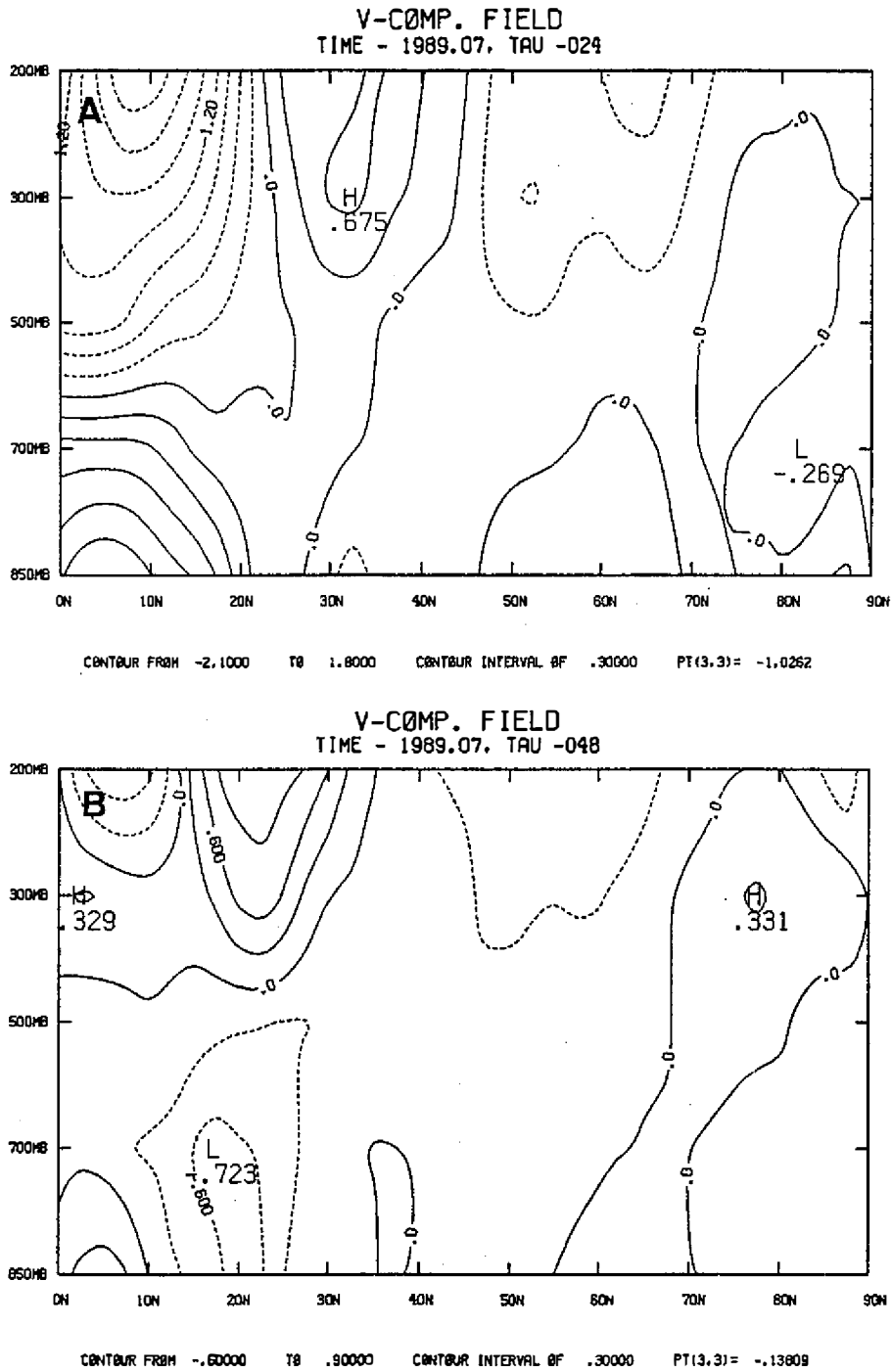


Fig. 16. Same as Fig. 11, except for July 1989. (a) day-1 forecast, (b) day-2 forecast.



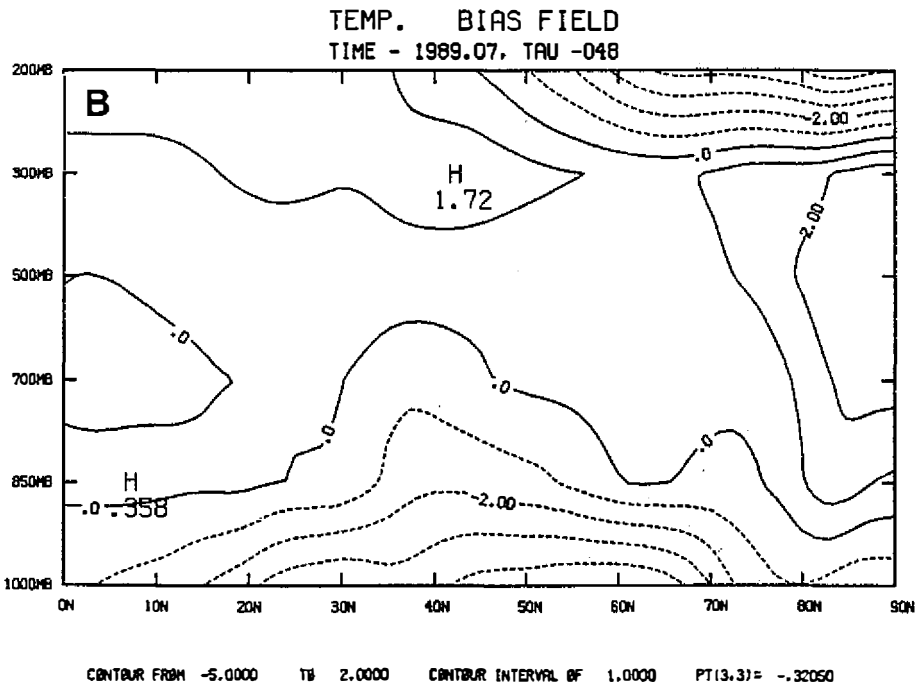
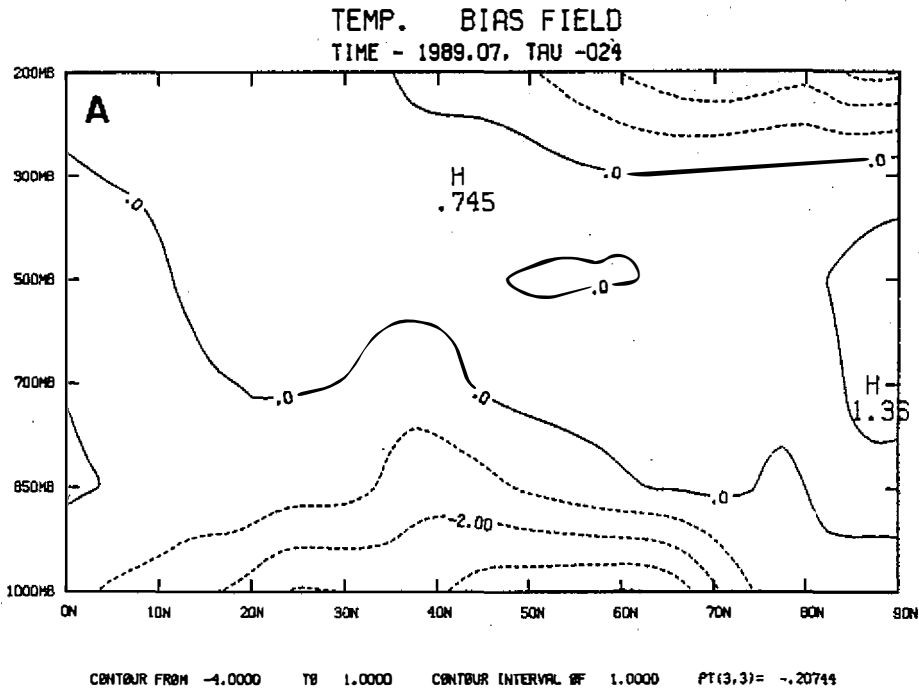


Fig. 18. The zonal mean of the temperature bias for January 1990. (a) day-1 forecast, (b) day-2 forecast.



Fig. 19. The simulated mean surface precipitation for January 1990. (a) day-1 forecast, (b) day-2 forecast, (c) day-3 forecast. The units are mm/day.

## REFERENCES

- Arakawa, A., 1966: Computational design for long-term numerical integrations of the equations of atmospheric motion. *J. Comput. Phys.*, **1**, 119-143.
- Arakawa, A., 1972: Design of the UCLA general circulation model. Numerical Simulation of Weather and Climate, Dept. of Meteorology, UCLA, Tech. Rept. 7, 116 pp.

- Arakawa, A., and V. R. Lamb, 1981: A potential Enstrophy and energy conserving scheme for the shallow water equations. *Mon. Wea. Rev.*, **109**, 18–36.
- Arakawa, A. and Y. Mintz, 1974: The UCLA atmospheric general circulation model. Notes distributed at the workshop, 25 March- 4 April, 1974, Dept. of Meteorology, UCLA, Los Angeles.
- Arakawa, A. and W.H. Schubert, 1974: Interaction of a cumulus cloud ensemble with the large-scale environment. Part I. *J. Atmos. Sci.*, **31**, 684–701.
- Arpe, K. and E. Klinker, 1986: Systematic errors of ECMWF operational forecasting model in middle latitude. *Quart. J. R. Met. Soc.*, **112**, 181–202.
- Brankovic, C., T. N. Palmer, F. Molteni, S. Tibaldi and U. Cubasch, 1990: Extended-range prediction with ECMWF models: Time lagged ensemble forecasting. *Quart. J.R. Meteor. Soc.*, **116**, 867–912.
- Bettge, T.W., 1983: A systematic error comparison between the ECWFM and NMC prediction models. *Mon. Wea. Rev.*, **111**, 2385–2389.
- Bourke, W., 1972: An efficient, one-level primitive-equation spectral model. *Mon. Wea. Rev.*, **100**, 683–689.
- Charney, J.G., R. Fjortoft, and J. von Neumann, 1950: Numerical integration of the barotropic vorticity equation. *Tellus*, **2**, 237–254.
- Cheng, M.-D., and M. Yanai, 1989: Effects of downdrafts and mesoscale convective organization on the heat and moisture budgets of tropical cloud clusters. Part IV: effects of convective downdrafts. *J. Atmos. Sci.*, **46**, 1566–1588.
- Johnson, R. H., 1984: Partitioning tropical heat and moisture budgets into cumulus and mesoscale components: Implications for cumulus parameterization. *Mon. Wea. Rev.*, **112**, 1590–1601.
- Kalnay, E., M. Kanamitsu and W.E. Baker, 1990: Global numerical weather prediction at the NMC. *Bull. Amer. Met. Soc.*, **71**, 1410–1428.
- Katayama, A., 1974: A simplified scheme for computing radiative transfer in the troposphere. Tech. Rep. No. 6, Dept. of Meteorology, UCLA, Los Angeles, 77pp.
- Kuo, H.L., 1974: Further studies of the parameterization of the influences of cumulus convection on large-scale flow. *J. Atmos. Sci.*, **31**, 1232–1240.
- Liou, C.-S., C.-T. Terng, W.-S. Kau, T.E. Rosmond, C.-S. Chen, J.-H. Chen and C.-Y. Tsay, 1989: Global forecast system at Central Weather Bureau. *P. Meteor. Res.*, **12**, 205–230.
- Pan, H.-L., 1990: A simple parameterization scheme of evapotranspiration over land for the NMC medium range forecast model. *Mon. Wea. Rev.*, **118**, 2500–2512.
- Phillips, N.A., 1956: The general circulation of the atmosphere: A numerical experiment. *Quart. J.R. Meteor. Soc.*, **82**, 123–164.
- Phillips, N.A., 1959: An example of non-linear computational instability. *The Atmosphere and the sea in motion*, Rossby Memorial Volume, Rockefeller Institute Press, 501–504.
- Richardson, L.F., 1922: *Weather Prediction by Numerical Process*. Cambridge University Press, reprinted Dover, 1965, 236 pp.

- Tibaldi, S, 1985: Envelope orography and maintenance of the quasi stationary circulation in the ECMWF global models. *Advanced in Geophysics*, **29**, 339–374.
- Wallace, J.M., S. Tibaldi and A.J. Simmons, 1983: Reduction of systematic forecast errors in the ECMWF model through the introduction of envelope orography. *Quart. J.R. Meteor. Soc.*, **109**, 683–717.
- Williamson, D.L., and R.E. Dickinson, 1976: Free oscillations of the NCAR global circulation model. *Mon. Wea. Rev.*, **104**, 1372–1392.
- Yanai, M., S. K. Esbensen, and J.-H. Chu, 1973: Determination of bulk properties of tropical cloud clusters from large-scale heat and moisture budgets. *J. Atmos. Sci.*, **30**, 611–627.